Carbohydrate Polymers 289 (2022) 119456

Contents lists available at ScienceDirect

Carbohydrate Polymers

journal homepage: www.elsevier.com/locate/carbpol

Injectable multifunctional hyaluronic acid/methylcellulose hydrogels for chronic wounds repairing

Linyu Long [a,1], Cheng Hu [a,1], Wenqi Liu [a], Can Wu [a], Lu Lu [b], Li Yang [a,*], Yunbing Wang [a,*]

[a] National Engineering Research Center for Biomaterials, Chuanda-Jinbo Joint Research Center, Sichuan University, Chengdu, 610064, China
[b] Key Laboratory of Medical Molecular Virology (MOE/NHC/CAMS), School of Basic Medical Sciences and Shanghai Public Health Clinical Center, Fudan-Jinbo Joint Research Center, Fudan University, Shanghai 200302, China

ARTICLE INFO

Keywords:
Multifunctional injectable hydrogels
Tissue adhesive
Antioxidant activity
Infected wound repair

ABSTRACT

Herein, an injectable multifunctional hydrogel based on dopamine grafted hyaluronic acid and phenylboric acid grafted methylcellulose was fabricated for promoting the repair of diabetic wounds. The prepared hydrogel possessed multifunctional properties including rapid gelation time (less than 10 s), self-healing, high water absorbency, tissue adhesiveness and excellent antioxidant activity. After loading Ag nanoparticles and the recombinant humanized collagen type III with high affinity to cells, the hydrogel exhibited properties of pH-/H_2O_2-responsive drug release profile, promoting cell proliferation and ideal antibacterial activity. Moreover, the *in vivo* experimental results demonstrated the prepared hydrogel could significantly accelerate wound repair by enhancing the collagen deposition and granulation tissue regeneration, reducing the expression of CD68 and improving the production of Ki67 and CD31 simultaneously. In conclusion, these multifunctional injectable hydrogels possessed great potential in chronic wound dressings.

1. Introduction

As the largest and the most exposed organ in human body, skin tissue is vulnerable to be damaged in burns, accidents, or surgery (S. Huang et al., 2020; Yongping Liang et al., 2019). Trauma to the skin tissue may destroy its protective barrier function, which makes the skin wound, especially diabetic wounds, prone to bacterial infection (S. Huang et al., 2020; H. Zhao et al., 2020). In addition, the excessive reactive oxygen species (ROS) generated at the infected wounds may improve the secretion of pro-inflammatory cytokines, resulting in irreversible cell damage, prolonged inflammation, and slow wound healing (Hussain et al., 2021; Yao et al., 2019; H. Zhao et al., 2020; Zhao, Wu, et al., 2017). Therefore, though most skin wound can be effectively and quickly repaired within 2 weeks, diabetic wounds infected with bacteria are usually difficult to repair, seriously affecting patients' health and even threatening human life.

Considering the complexity of the chronic wounds repair, the ideal wound dressing should possess multiple functions, which can effectively reduce inflammation, promote angiogenesis, inhibit bacterial infection and promote tissue regeneration (Ahmadian et al., 2021; Gao et al., 2020; Yongping Liang et al., 2019; Xu et al., 2020). So far as we know, various biomaterials including decellularized biological tissues, nanofibers, hydrogels and sponges have been developed for promoting the effective repair of chronic wounds (Cao et al., 2021; Zhang et al., 2021; Zhao, Niu, et al., 2017). It is worth noting that hydrogel dressings have attracted extensive attention from researchers among these dressings because of their advantages of maintaining a moist environment and absorbing tissue exudate (Chen et al., 2018; He et al., 2020; Li, Fu, et al., 2021; Zheng et al., 2020). Especially, injectable polymeric hydrogels have become a more promising option due to their unique features of convenient clinical operation, soft mechanical strength similar to extracellular matrix (ECM), *in situ* encapsulating drugs, seamless filling the irregular shaped wound, adjustable physical and chemical properties (Gao et al., 2020; Li, Cao, et al., 2021; Qu et al., 2018; Wang et al., 2019; H. Zhao et al., 2020). However, it's still an unmet prerequisite to develop a wound dressing that can effectively prevent bacterial infections, remove excessive ROS, and promote extracellular matrix remodeling.

Due to its functions of mediating cellular signaling and promoting cell migration, hyaluronic acid (HA), a natural polysaccharide, has been widely applied in various biomedical fields including wound dressings, dermal fillers and tissue engineering (Koivusalo et al., 2019; Suo et al., 2021; Yu et al., 2020). Besides, HA also has many properties including

* Corresponding authors.
E-mail addresses: yanglisc@scu.edu.cn (L. Yang), yunbing.wang@scu.edu.cn (Y. Wang).
[1] These authors contributed equally to this work.

https://doi.org/10.1016/j.carbpol.2022.119456
Received 19 December 2021; Received in revised form 17 March 2022; Accepted 31 March 2022
Available online 4 April 2022
0144-8617/© 2022 Published by Elsevier Ltd.

biodegradability, active chemical property and biocompatibility which are beneficial to design and fabricate injectable hydrogel (Hwang et al., 2021; Yongping Liang et al., 2019). Herein, we prepared dopamine (DA) grafted HA (HA-DA) by grafting DA onto the molecular chain of HA *via* amide bonds. As we all know, the presence of physical bonding and chemical cross-linking between soft tissues and catechol groups make the hydrogels containing catechol group generally have wet adhesion to soft tissues (Shan et al., 2017; Teng et al., 2021). The good tissue adhesion will enable hydrogels to prevent the wound from cracking again (Xiong et al., 2021). And at the same time, the tissue adhesive hydrogels can also effectively reduce the risk of bacterial infection by acting as a sealant (Teng et al., 2021; Xiong et al., 2021). In addition, the hydrogels containing catechol group also have antioxidant capacity, thereby accelerating the repair of chronic wound by adjusting the oxidative stress level at the wound site (Yongping Liang et al., 2019; Xu et al., 2020).

As shown in Fig. 1, an injectable hydrogel with self-healing performance, antibacterial, antioxidant activity and tissue adhesion by using HA-DA and phenylboric acid grafted methylcellulose was developed. After loading the silver nanoparticles (AgNPs) with broad-spectrum antibacterial properties (Wu, Zhou, et al., 2020; Yu et al., 2020) and the recombinant humanized collagen type III (rhCol III) with high affinity to cells (Yang, Wu, et al., 2021), the prepared dual-crosslinked hydrogel exhibited various properties of pH-/H_2O_2-responsive drug release profile, promoting cell proliferation and good antibacterial activity. Based on the active peptide sequence of human type III collagen, the tailored rhCol III with a stable triple-helical conformation retains fragments of high cellular activity (Gly-Glu-Arg (GER) and Gly-Glu-Lys (GEK) triad). Most importantly, the immune and rejection reactions of this rhCol III are much milder compared with animal-derived collagen, and it has good water solubility (Yang, Wu, et al., 2021). In addition, the prepared biocompatible hydrogel also showed rapid gelation time (less than 10 s), self-healing ability, high swelling ratio, bio-adhesiveness, and free radical scavenging capacity.

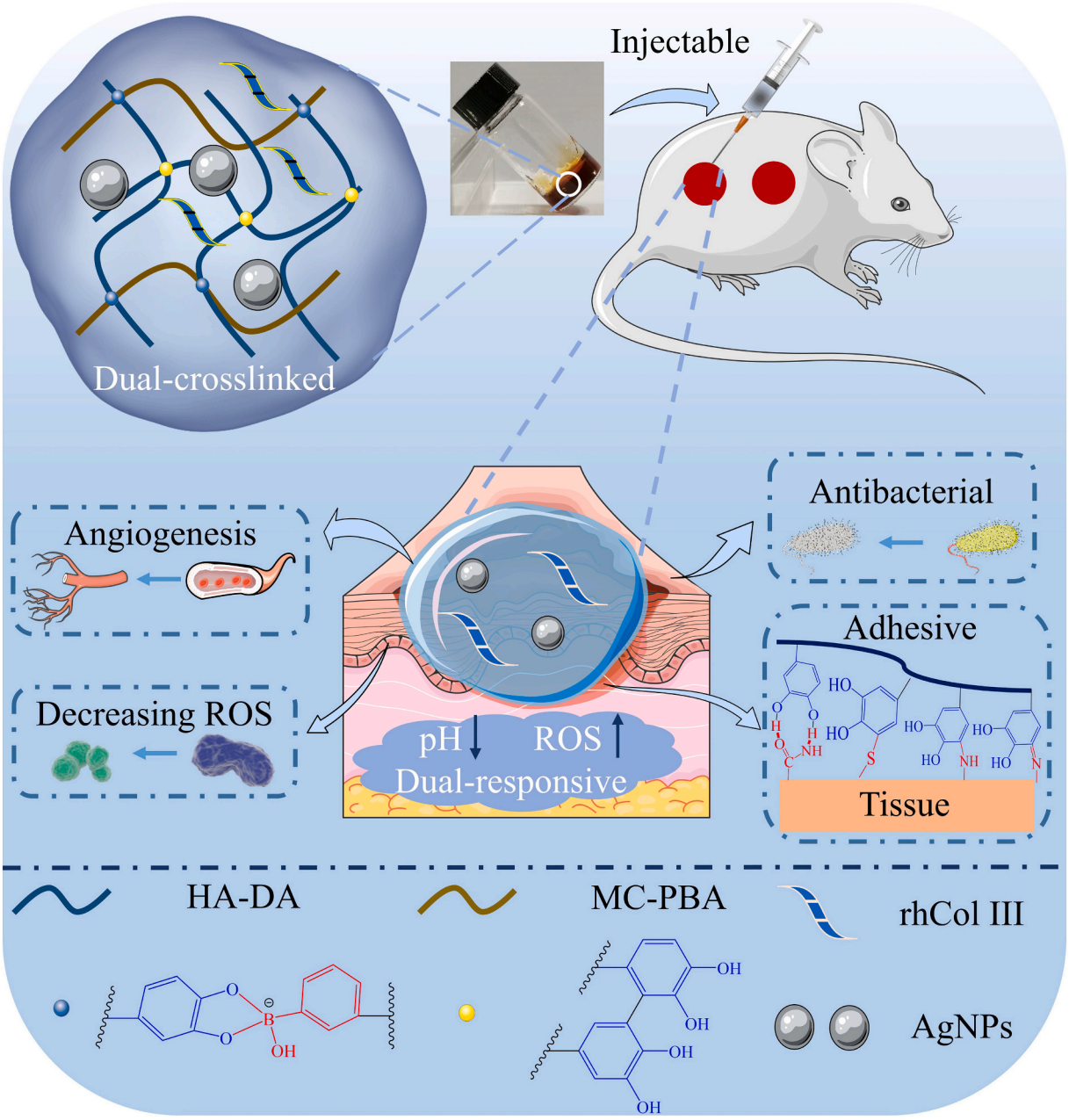

Fig. 1. Schematic presentation of preparation and functions of injectable multifunctional hydrogel.

Moreover, the excellent promoting effects in chronic wound repair of these multifunctional hydrogels were demonstrated by wound closure, histomorphological examinations, and immunofluorescence staining in a diabetic rat full-thickness skin wounds model.

2. Materials and methods

2.1. Materials

N-(3-dimethylaminopropyl)-N′-ethylcarbodiimide hydrochloride (EDC.HCl; ≥98%), N-hydroxysuccinimide (NHS; 98%), trisodium citrate (≥99%), and hyaluronic acid (HA; molecular weight (MW) =10 kDa; ≥96%) were purchased from Sigma-Aldrich (Saint Louis, MO, USA). Dopamine hydrochloride (DA; ≥98%), methyl cellulose (MC; ≥95%) and 3-aminophenylboronic acid (APBA; ≥99%), 1,1-diphenyl-2-picryl-hydrazyl (DPPH; ≥97%) was purchased from Shanghai Macklin Biochemical Co., Ltd. (Shanghai, China); Sodium borohydride (≥98%), silver nitrate (≥99.8%) and sodium periodate (≥99.8%) were purchased from Shanghai Titan scientific Co., Ltd. (Shanghai, China); Tailored rhCol III (≥95%) was prepared by Shanxi Jinbo Bio-Pharmaceutical Co., Ltd. (Taiyuan, China), and the preparation process was the same as previously reported method (Yang, Wu, et al., 2021). rhCol III is composed of 16 tandem repeats of the triple-helix fragment. The tandem repeats peptide contains the sequence of high cytoactive, derived from the Gly_{483}-Pro_{512} sequence of the human type III collagen.

2.2. Preparation of DA grafted HA (HA-DA)

HA-DA was prepared by using the method reported previously (Koivusalo et al., 2019; Yongping Liang et al., 2019). The details were available in the Supporting Information (SI) Methods. The yield was calculated taking into account that the introduction of each DA group caused an increase of 135 g mol^{-1} and using the formula reported previously (Huerta-Angeles et al., 2014; Huerta-Angeles, Brandejsová, Kulhánek, et al., 2016).

2.3. Preparation of APBA grafted oxidized MC (OMC-PBA)

Firstly, MC was oxidized with sodium periodate to obtain OMC. And The OMC-PBA was synthesized by using the Schiff bond reaction between the aldehyde group of OMC and the amino group of APBA. The details were available in the SI Methods. The yield was calculated using the method described in Section 2.2.

2.4. Preparation and characterization of HA-DA/OMC-PBA hydrogels

In Brief, 100 mg of HA-DA was dissolved in 1 ml of AgNPs suspension (30 μg/ml). And the resulting solution was gradually mixed with 1 ml of OMC-PBA (10 wt%) and rhCol III (4 mg) composite solution (pH = 8.5). The mixture was allowed to stand for 30 s to obtain hydrogel. According to the addition of AgNPs or rhCol III, the hydrogels were named as H-C, H-Ag, H-III and H-Ag/III and stored at 4 °C for further use. The characterizations of the hydrogels were available in the SI Methods.

2.5. Adhesive strengths of hydrogels

The tissue adhesive strength of the prepared hydrogels for fresh porcine skin was measured by the lap-shear strength test as previously reports described (J. Huang, Jiang, et al., 2021; J. Huang, Liu, et al., 2021; Tang et al., 2020). The details were available in the SI Methods.

2.6. Antioxidant ability of hydrogels

The antioxidant ability of the HA-DA based hydrogels was assessed by measuring the efficiency of scavenging the stable DPPH free radical (Yongping Liang et al., 2019). The details were available in the SI Methods.

2.7. Ag^+ and rhCol III release of hydrogels

The cumulative release of Ag^+ and rhCol III were tested at pH 7.4 or pH 5.0, with or without 100 μM H_2O_2. The details were available in the SI Methods.

2.8. In vitro biocompatibility studies

The cell experiments *in vitro* were performed by incubating the hydrogel extracts with the mouse fibroblast L929 cells (Hu et al., 2021). The details were available in the SI Methods.

2.9. Antibacterial performance of the hydrogels

The antibacterial performance of hydrogels was conducted by using culture turbidity as the qualitative measure of bacterial growth against *S. aureus* and *E. coli*. The details were available in the SI Methods.

2.10. In vivo wound healing performance

All animal studies were conducted according to our previous report (Hu et al., 2020a; Hu et al., 2021; Long et al., 2022) and approved by the animal research committee of Sichuan University. The details were available in the SI Methods.

2.11. Statistical analysis

The results of statistical analysis of all experimental data were expressed as mean ± standard deviation. Statistical differences were determined using Student's *t*-test, ANOVA test and chi-square test, and differences were considered significant if $P < 0.05$.

3. Results and discussion

3.1. Synthesis of HA-DA and OMC-PBA polymer

In this paper, HA was selected as one of the main components of the hydrogel. For the purpose of introducing the properties of antioxidant and tissue adhesion to enhance the capacity of hydrogels to promote wound repair, DA was linked to the HA molecular chain *via* the EDC/NHS chemistry (Fig. 2A). The successful preparation of HA-DA was verified by FT-IR analysis. In the FT-IR spectrum of HA-DA, it could be observed that peak for O—H stretching appeared at 3286 cm^{-1}, peak for C—H stretching in the pyranose ring appeared at 2917 cm^{-1}, and peak for C═O stretching in amide bond appeared at 1643 cm^{-1} (Fig. S1) (Hwang et al., 2021). The successful conjugation of DA to HA was further determined by using ^1H NMR analysis (Fig. 2B). As shown in Fig. 2B, 3 new peaks appeared at 6.7 ppm illustrating a phenyl ring in dopamine, and the proton peak at 2.76 ppm was because of the —CH_2— group closed to the catechol ring (Hwang et al., 2021; Koivusalo et al., 2019; Lee et al., 2021; Yongping Liang et al., 2019; Zheng et al., 2020). In addition, since the diffusion coefficients of dopamine with low molecular weight and HA with high molecular weight are significantly different, diffusion ordered NMR spectroscopy (DOSY) can be used to further confirm the successful grafting of dopamine molecules to the HA molecular chain (Huerta-Angeles et al., 2017; Huerta-Angeles, Brandejsová, Knotková, et al., 2016). As displayed in Fig. S2, dopamine and HA possessed similar diffusion coefficients, suggesting that all proton signals in this region belonged to one structural complex. And the content of catechol group was determined by UV–vis. As illustrated in Fig. S3, the degree of dopamine substitution for HA-DA was 8.4% according to the standard curve of dopamine. As the introduction of each dopamine group caused an increase of 135 g mol^{-1}, the yield of HA-DA could be calculated to be 96.7%. In conclusion, a high-purity HA

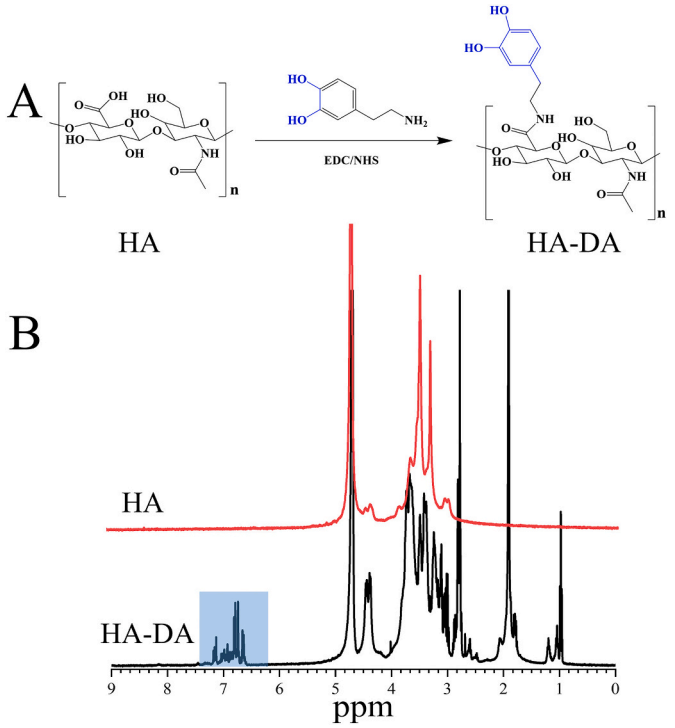

Fig. 2. (A) The Synthesis process of HA-DA. (B) ^{1}H NMR (D_2O) spectra of HA and HA-DA.

derivative, HA-DA, was successfully synthesized here.

Previous studies have shown that boric acid and glycol can be covalently bonded in alkaline environment, while boronate-ester crosslinked hydrogels are likely to decompose into various reactants under acidic conditions or high ROS (Hu et al., 2020b; Lee et al., 2021). Herein, OMC-PBA, which was prepared based on the aldehyde group of OMC and the amino group of APBA (Fig. 3A), was selected as another component of the hydrogel. To better demonstrate the oxidation process of MC, only one distribution of methoxy groups was given here. The successful preparation of OMC-PBA was also verified by FT-IR, ^{1}H NMR and UV–vis. In FT-IR spectra, peak at 1742 cm^{-1} indicated the carbonyl group stretch of aldehyde groups of the OMC and OMC-PBA (Fig. S4) (Aydemir Sezer et al., 2019; Tsai et al., 2021) And an O—B—O bend was observed at 1354 cm^{-1} in the spectrum of OMC-PBA (Lee et al., 2021). In addition, the ^{1}H NMR further demonstrated the successful synthesis of OMC-PBA. As illustrated in Fig. 3B, proton chemical shifts at 7.2–7.8 ppm illustrated the existence of a phenyl ring group (in APBA) (Lee et al., 2021). Additionally, the DOSY experiment further confirmed that APBA molecules were successfully grafted onto OMC molecular chains (Fig. S5). The content of APBA in OMC-PBA was 13.2% calculated from the results of UV–vis (Fig. S6). And the yield of OMC-PBA could be calculated to be 92.8%. Overall, a high-purity MC derivative, OMC-PBA, was successfully synthesized.

3.2. Preparation and performances of hydrogels

The tilting test is usually used to investigate the gelation behavior of designed hydrogel systems. Herein, the dual-responsive hydrogel with tissue adhesive property was fabricated within 10 s by mixing the HA-DA solution (pH = 7.4) and CMC-PBA solution (pH = 9.0) (Fig. 4A). Hydrogels formed by dynamic boronate ester bonds possessed the injectable performance and self-healing property (Lee et al., 2021; Tsai et al., 2021). In biomedical applications, injectability is a key performance for minimally invasive and topical delivery of therapeutic hydrogels (Wu, Chen, et al., 2020). As shown in Fig. 4B, the hydrogels could be injected by a syringe to write "☆" without any clogging,

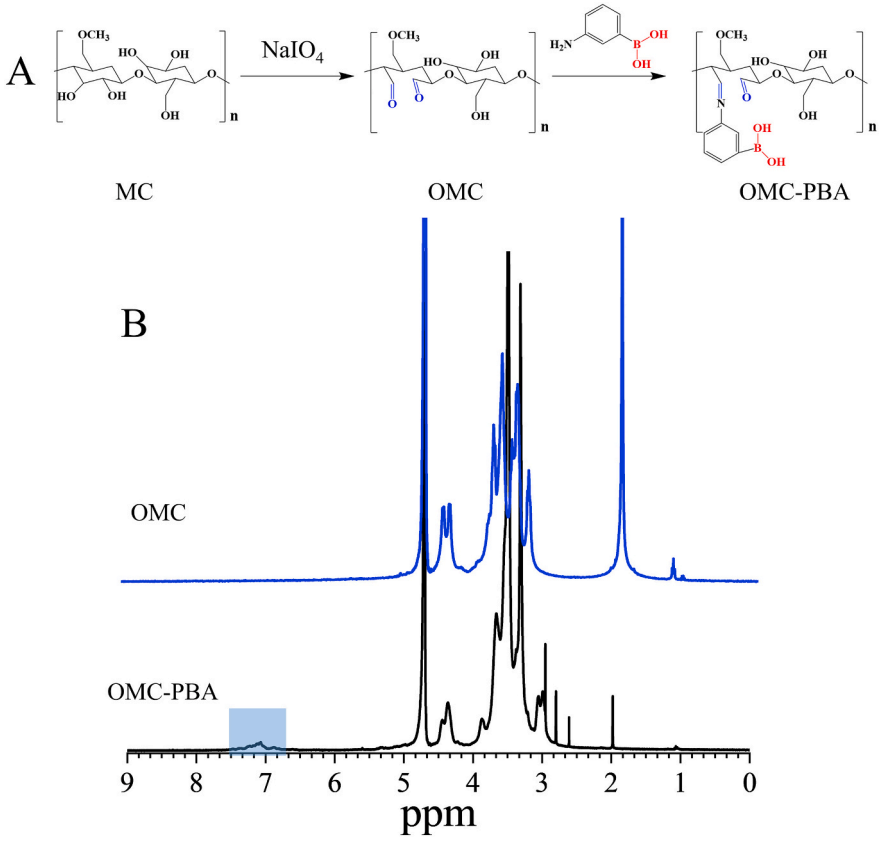

Fig. 3. (A) The Synthesis process of OMC-PBA. (B) ^{1}H NMR (D_2O) spectra of OMC and OMC-PBA.

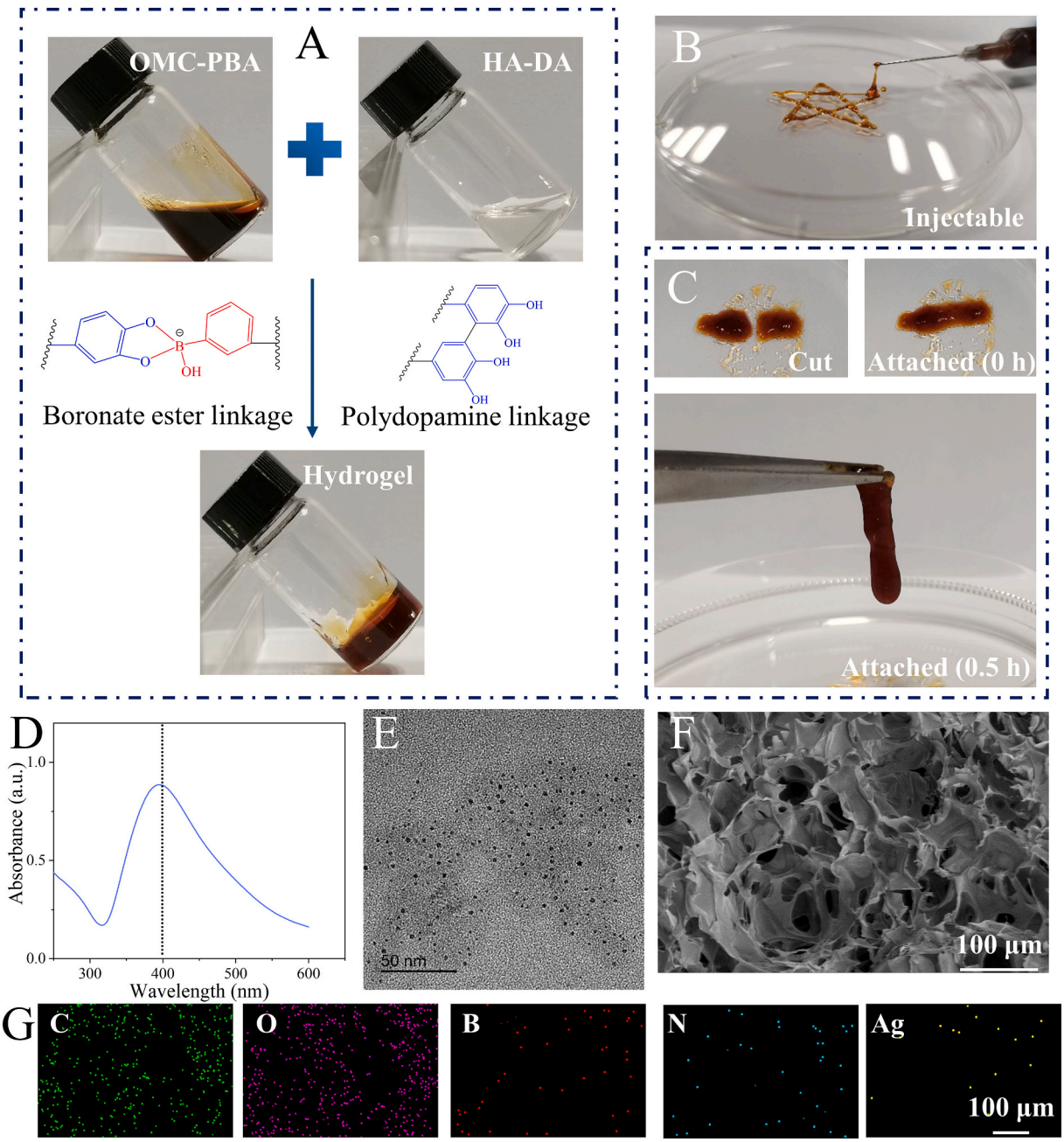

Fig. 4. (A) Photograph of the final hydrogel, which was formed within 10 s by mixing 10 wt% HA-DA and 10 wt% CMC-PBA solutions at pH 8.5. Pictures of the injectability (B) and self-healing (C) of hydrogel. UV–Vis spectra (D) and TEM image (E) of AgNPs. SEM images (F) and EDS-mapping (G) of freeze-dried H-Ag/III.

illustrating their good injectability. In addition, two pieces of hydrogel could adhere together after 0.5 h of contact and the healed hydrogel could be picked up with tweezers (Fig. 4C), indicating their self-healing property. When applied to wounds, the self-healing ability ensure the hydrogel can still prevent liquid leakage, bacterial penetration and infection even when the hydrogel is deformed or broken due to external forces (Yongping Liang et al., 2019; Liu et al., 2020).

Antibacterial AgNPs were prepared and embedded into the hydrogel network by mixing suspension of AgNPs with hydrogel precursors during the gel crosslinking process. Herein, AgNPs were synthesized by $NaBH_4$ reduction. As displayed in Fig. 4D, the maximum UV–vis absorption peak appeared at ~396 nm, illustrating the successful synthesis of the AgNPs (Khamrai et al., 2019; Lin et al., 2021; Zhong et al., 2020). And the TEM image of AgNPs indicated the size of AgNPs ranging from 6 nm to 25 nm with an average particle size of ~14 nm (Fig. 4E).

The porous structure of hydrogel facilitates the transportation of nutrients and prevents leakage of body fluids (S. Huang et al., 2020). The surface morphologies of the hydrogel were detected by scanning electron microscope (SEM). As illustrated in Fig. 4F, the hydrogel showed an interconnected porous structure with homogeneous circular pores. And the EDS-mapping also detected the carbon, oxygen, nitrogen, silver and boron elements were uniformly distributed in the H-Ag/III (Fig. 4G). And the hydrogel with strong water uptake capacity can accelerate wound repair *via* removing wound effluence and reducing the risk of infection (Yongping Liang et al., 2019). The swelling behavior of these prepared hydrogels under different pH was displayed in Fig. S7. In general, hydrogels reached the maximum water absorption rate of their initial weight (≈270%) after 3 d in PBS (pH 7.4). In an acidic environment, the swelling ratio of the hydrogel was about 162%. And with the extension of time, the structure of the hydrogel gradually disintegrated,

resulting in a decrease in the swelling rate. And the results of the degradation experiments of the hydrogels within 14 days showed that the hydrogels degraded faster in the presence of acidity (pH = 5.0) and H_2O_2 than in the neutral environment (Fig.S8). Overall, the prepared hydrogels with large water absorption and interconnect porous structure could absorb wound exudates and transmit nutrients/metabolites, thereby promoting wound repair (Teng et al., 2021).

3.3. Rheological performance and drug release profile of hydrogels

The wound dressing based on self-healing hydrogels can relieve damage from external physical force after being applied to the wound site, thereby prolonging their lifespan (Zhao, Wu, et al., 2017). The rheology test was conducted to further measure the self-healing performance of these prepared hydrogels. The strain amplitude sweep of the H-C and H-Ag/III showed their hydrogel network would collapse when 500% strain was applied. As illustrated in Fig. 5A, when the 500% strain was applied, the storage modulus (G′) of the H—C decreased remarkably from 378 to 60 Pa, while the G′ of the H-Ag/III decreased significantly from 402 to 62 Pa. In addition, the loss modulus (G″) of the H—C and H-Ag/III were greater than their G′, illustrating the hydrogels network had collapsed. After the low strain (1%) was applied, the G′ of the H—C and H-Ag/III recovered more than 80% and their G′ were both greater than G″, illustrating that crosslinking of hydrogels was partially recovered. The above results demonstrated the self-healing performance of the prepared hydrogels formed by dynamic boronate ester bonds.

Phenylborate ester formed by phenylboric acid and vicinal diol is not stable under acidic conditions and high ROS (Lee et al., 2021; Shan et al., 2017). To analyze the influence of pH and H_2O_2 on the rheological performance of hydrogels, the curves of G′ and G″ of these hydrogels treated with HCl (for pH adjustment to 5.0) or H_2O_2 (100 μM) over time were recorded. As shown in the images in Fig. 5B, the addition of HCl or H_2O_2 would induce disintegration of the hydrogel structure based on boronate ester bonds. The untreated hydrogel could stay at the bottom of the inverted plastic tube, while the hydrogel treated with HCl and H_2O_2 couldn't. And the G′ of hydrogel at pH = 7.4 (398.6 Pa) was higher than hydrogels treated with HCl (71.5 Pa) or H_2O_2 (90.1 Pa). Moreover, the G′ of hydrogel treated with HCl and H_2O_2 was only 0.002 Pa, which was lower than their G″ (26.5 Pa). Overall, acidification or the addition of oxidants (H_2O_2) might induce the dissociation of hydrogel structure.

Due to the acidic microenvironment and high ROS level in the wound site, drug-loaded pH-/H_2O_2- responsive hydrogel was capable of

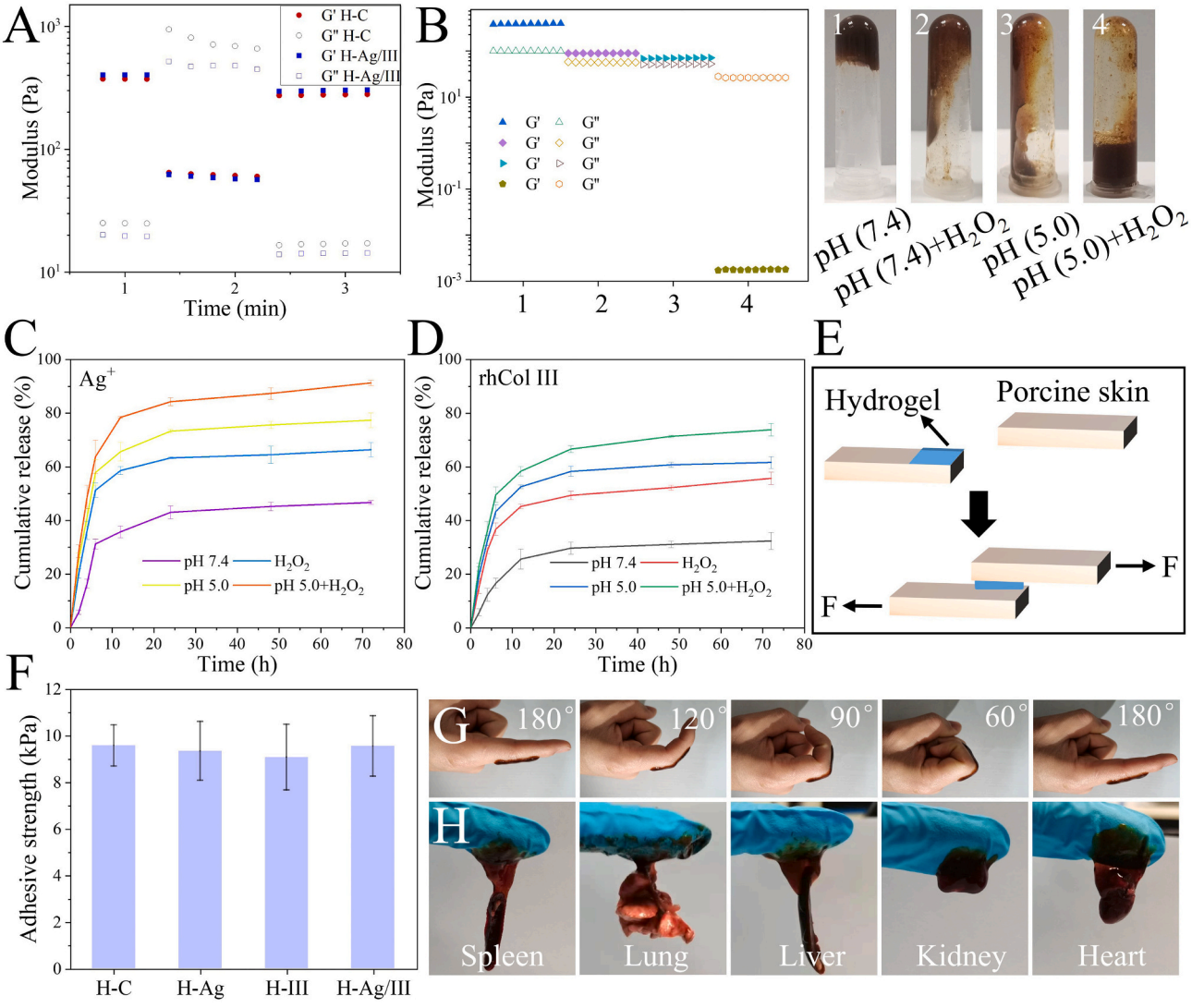

Fig. 5. (A) Step-strain sweep of hydrogels at a small strain of 1% and a large strain of 500%. (B) Rheological analysis (left) and images (right) of hydrogel at pH = 7.4 and pH = 5.0 with or without H_2O_2 (100 μM).The drug cumulative release of the hydrogel at different time points: (C) Ag^+; (D) rhCol III. (E) Schematic illustration of the lap-shear adhesion test of hydrogels. (F) The adhesion strength of the hydrogels to the porcine skin (n = 3). Photos of the tissue adhesion of the hydrogels to the finger (G) and rat tissue surface (H).

achieving wound microenvironment responsive drug release.(Shen et al., 2021) The release profiles of Ag^+ and rhCol III from hydrogels in PBS were measured at pH 5.0 and 7.4 with and without H_2O_2 (100 μM), and results were displayed in Fig. 5C and D. Compared to the PBS group, there rapid release of Ag^+ (1.95 times) and rhCol III (2.28 times) could be detected at pH = 5.0 with 100 μM H_2O_2 in the first 6 h. The rapid release of Ag^+ at the acidic and oxidative condition enabled the prepared hydrogel to specifically shorten inflammatory phase, thereby promoting the wounds repair process.

3.4. Adhesive property and antioxidant ability of hydrogels

Tissue adhesion is one of the most critical properties for hydrogel wound dressings. Adhesive hydrogels are capable of sticking to biological tissue to prevent the wound from cracking again and protect the wound from the damage caused by external forces. (Shen et al., 2021; Xiong et al., 2021). Moreover, adhesive hydrogels can reduce fluid or gas leakage from the tissue, prevent bacterial infection by serving as physical barrier, or sealant (He et al., 2020; Li, Cheng, et al., 2021; Shen et al., 2021; Zhao, Wu, et al., 2017). It is noted that the catechol groups in the hydrogel skeleton molecules (including oxidized o-quinone moieties) could form covalent bonds with the thiols, hydroxyl and amine groups on the surface of biological tissue (Teng et al., 2021; B. Yang et al., 2020; D. Zhou et al., 2020). The tissue-adhesive properties of the hydrogels to porcine skin were evaluated by using the lap shear test (Fig. 5E). As shown in Fig. 5F, the adhesion strength of all hydrogels to porcine skin tissue exceeded 9 kPa. And the hydrogel remained tightly adhered to the finger, even when the finger was bent from 0° to 120° (Fig. 5G). Additionally, the hydrogel on the finger was capable of adhering to the surface of rat organs (including heart, liver, spleen, lung, kidney) tightly and would not fall off after being lifted up, which illustrated the prepared hydrogels possessed good tissue adhesion (Fig. 5H).

Excessive ROS at the wound site may hinder angiogenesis and tissue regeneration or even endanger wound repair, especially in chronic wounds (Ahmadian et al., 2021; Hussain et al., 2021; Shen et al., 2021; Xu et al., 2020). Studies of the introduction of antioxidant function to wound dressing have been verified to remarkably accelerate chronic wound repair (M. Li et al., 2020; Qu et al., 2018, Qu et al., 2019; Zhao,

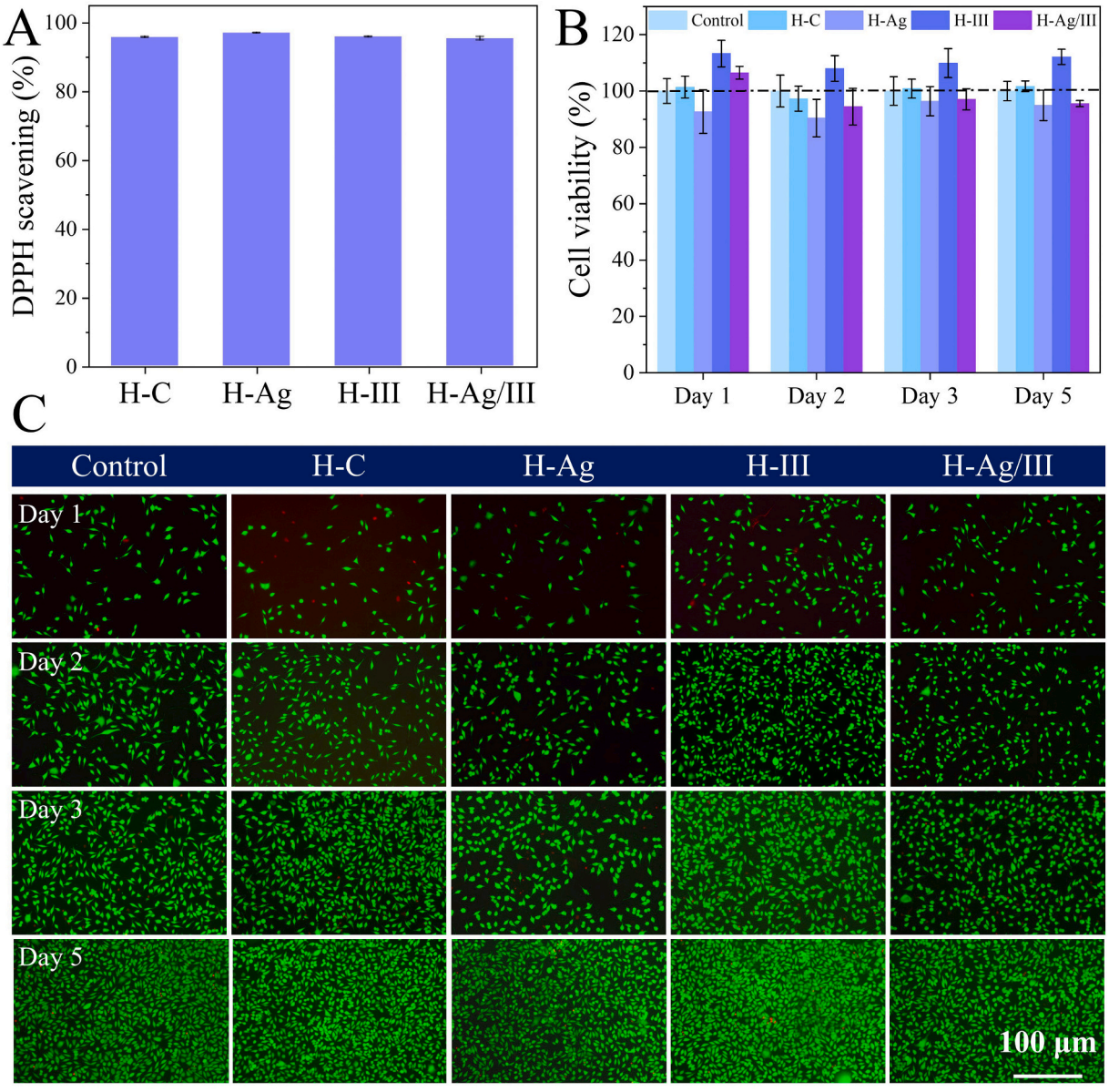

Fig. 6. (A) DPPH scavenging percentage by four hydrogels. (B) Cell viability of the L929 cells incubated with the different hydrogels extracts. (C) Live/dead staining of L929 cells after incubation with the hydrogels extracts for 1, 2, 3, 5 days.

Wu, et al., 2017). The antioxidant ability of the prepared hydrogels was assessed by measuring their efficiency for scavenging the stable free radical DPPH. As shown in Fig. 6A, 5 mg/ml of the hydrogel could scavenge more than 95% of free radicals. In conclusion, the above results proved that the prepared hydrogels possessed good antioxidant capacity which increased their ability to promote chronic wound repair.

3.5. Evaluation of the hydrogels' cytocompatibility

To evaluate the cytocompatibility of hydrogels, a hydrogels leaching test was conducted (Yuqing Liang et al., 2021; X. Zhao et al., 2018). As shown in Fig. 6B, the L929 cells viability of four groups was >80% after incubation with hydrogels leach liquor for 1, 2, 3, 5 days, indicating the good biocompatibility of the prepared hydrogels. After 5 days of co-incubation, the number of cells in H-III group was higher than that in the control and H-C groups. In addition, the pictures of the cells live/dead staining in Fig. 6C showed there were more cells observed after 5 days than 1 day, indicating L929 cells grew and proliferated throughout the experiment. And the H-III group possessed the highest fluorescence intensity in all five groups, illustrating the promoting effect of rhCol III on cell proliferation. Collectively, the above results confirmed the prepared hydrogels possessed good biocompatibility, indicating their wide application prospects in wound dressing for bacteria-infected wound therapy.

3.6. Antibacterial activity of hydrogels

Since the bacterial infections may cause inflammation, increase exudate formation and hinder the wound repair process, antimicrobial property is crucial for an ideal wound dressing (Shen et al., 2021). However, it is still a challenging task to design wound dressing that can efficiently and safely inhibit toxic bacterial strains. Herein, *S. aureus* and *E. coli* which are two of the most common colonized biofilms in the chronic wound tissue were selected to assess the antibacterial performance of the prepared hydrogels *in vitro* (Ahmadian et al., 2021). And the antibacterial activities of hydrogels were investigated through OD_{600} values and standard spread plate method. As shown in Fig. 7A and B, the final OD value after co-cultivation of the bacterial suspension and the hydrogel extract for 24 h was detected to assess the antibacterial performance of hydrogels. Turbid media were observed in the control group, H-C and H-III treated groups, revealing a rapid bacterial growth. In contrast, bacterial growth was remarkably suppressed in the groups treated with H-Ag and H-Ag/III. As shown in Fig. 7C, the number of colony forming units (CFUs) in groups treated with H-Ag and H-Ag/III was remarkably less than that in control group, indicating a significant inhibition of bacterial proliferation. The excellecnt antibacterial activity of hydrogels was attributed to the deposition of AgNPs, a well-known broad-spectrum antibacterial material, which could effectively inhibit the growth of bacteria. (Cao et al., 2021; Lin et al., 2021; Yu et al., 2020).

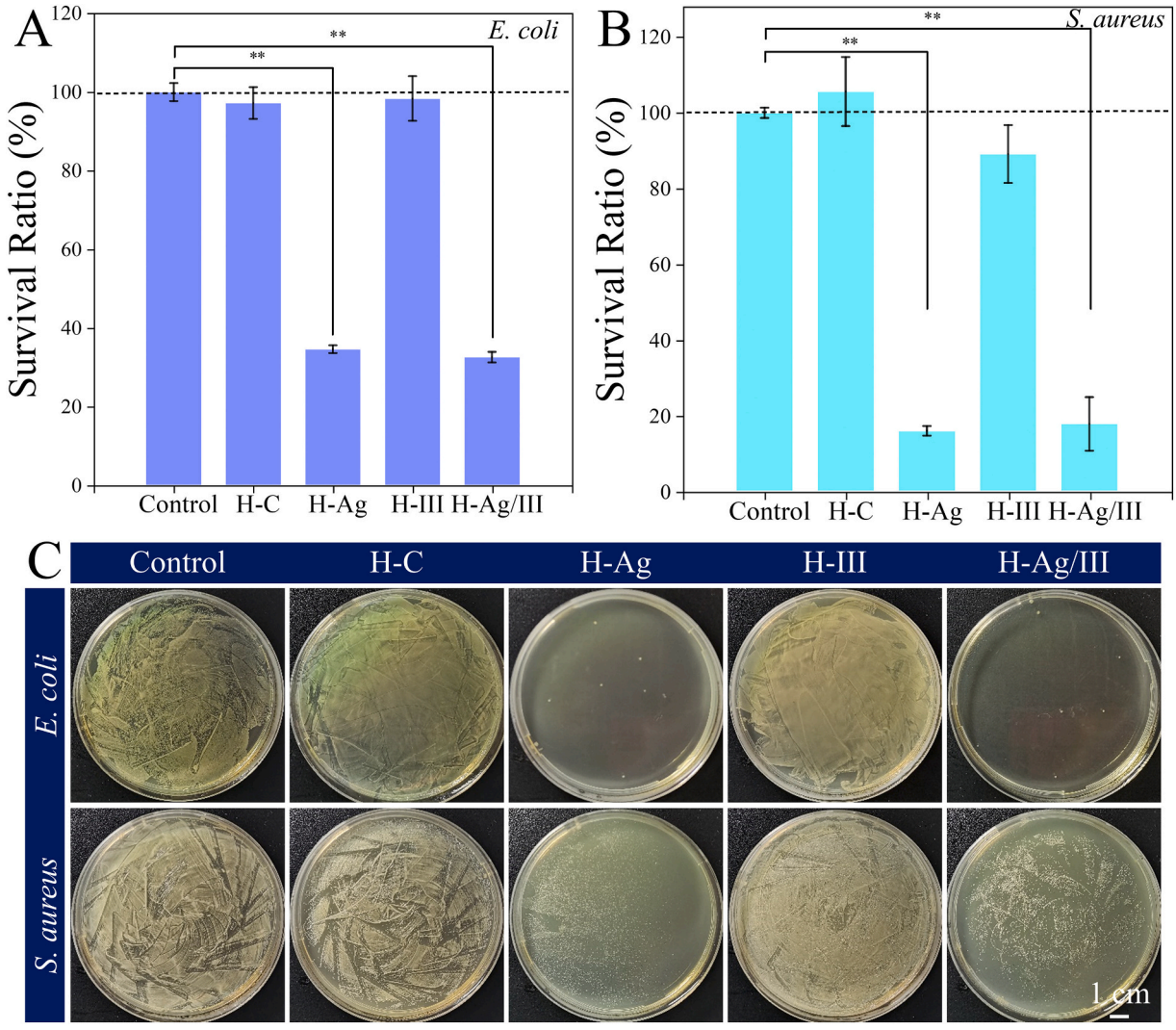

Fig. 7. Optical density (600 nm) values of bacterial solutions after incubation with hydrogel extracts for 12 h: (A) *E. coli*, (B) *S. aureus*. (mean ± SD, $n = 6$, $^{**}P < 0.01$). (C) Bacterial clones of *E. coli* and *S. aureus* with hydrogel leaching.

In conclusion, the AgNPs decorated hydrogels exhibited great potential to efficiently protect wound from bacterial infection.

3.7. In vivo wound repair efficacy

The advantages of the prepared hydrogels as a wound dressing were confirmed by using a diabetic bacterial-infected rat model to further evaluate the ability of hydrogels to promote wound repair *in vivo*. After receiving various treatments, the representative photographs of wound closure at 5th, 7th and 14th days were displayed in Fig. 8A. As illustrated in Fig. 8B, as the postoperative time increased, the wound area of all five groups became smaller. After 5 days of treatment, the wound area of the H-Ag/III group was smaller than that of the other four groups. The wound area of rats in H-Ag/III group decreased to 40.32%, while the wound areas of rats in control, H-C, H-Ag and H-III groups were 83.43%, 76.25%, 53.36% and 46.64%, respectively. After being treated for 7 days, the H-Ag/III group still exhibited remarkably faster wound repair rate than control group. After being treated for 14 days, the wounds treated with H-Ag/III showed completely closed and became smooth with regenerated epidermal tissue, and even some of the rats displayed hair coverage. Whereas 15.48% and 13.36% of wounds remained open with uneven scars in control and H-C groups, respectively, which indicated the H-Ag/III was intrinsically beneficial to wound healing. Bacteria from the wounds were collected after 7 days of treatment and diluted 10^5 times. As indicated in Fig. S9, the antibacterial effect in the H-Ag and H-Ag/III groups were more significant than that in the other groups, indicating the AgNPs decorated hydrogels could effectively eliminate bacterial infection. All these *in vivo* results illustrated the H-Ag/III possessed great promoting effect in wound repair, which might be attribute to the combined effects of the H-Ag/III hydrogel in anti-oxidation, antibacterial, cell proliferation, anti-inflammatory, angiogenesis and inducing ECM formation.

To further confirm this conclusion, hematoxylin and eosin (H&E) staining and Masson's trichrome staining were performed after 7 and 14 days of treatment (Fig. 8C and D). H&E staining was usually conducted to evaluate granulation tissue formation. In the H&E staining, compared

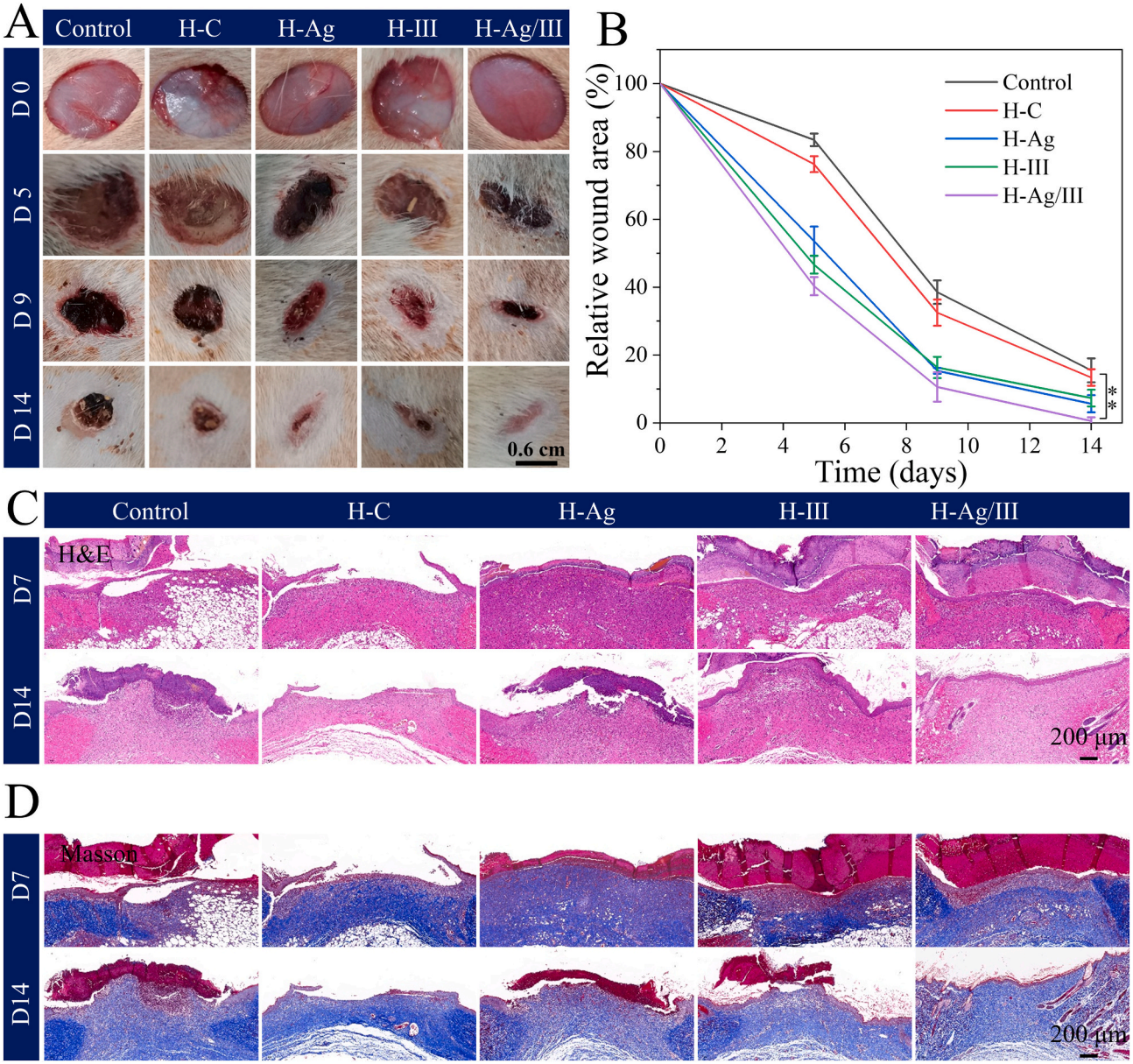

Fig. 8. (A) Representative photographs of the wounds treated with different samples. (B) Relative wound area on day 5, 9, and 14. (mean ± SD, $n = 6$, $^{**}P < 0.01$) H&E-staining (C) and Masson trichrome staining (D) results of skin tissues at determined times.

with the H-Ag/III groups, significant tissue destruction and inflammatory cell infiltration were observed in the control group on days 7 and 14. Additionally, the Masson's trichrome staining was conducted to evaluate the collagen deposition and distribution.(Zhao, Niu, et al., 2017; L. Zhou et al., 2021) The results of Masson's trichrome staining indicated there were intact epidermis, higher-ordered collagen fibers, and mature hair follicles in the H-Ag/III group on days 7 and 14. While a few collagen fibers and plenty of granulation tissues were observed in the skin tissues of control and H-C groups. These results of H&E and Masson's trichrome staining suggested that the injectable multifunctional hydrogel could improve the efficiency of diabetic infected wound repair by promoting the wounds re-epithelialization and increasing collagen deposition.

3.8. CD68, Ki67 and CD31 expression during the healing process

Moreover, the mechanism of the prepared hydrogel promoting wound repair was verified by CD68, Ki67 and CD31 immunofluorescence staining (Fig. 9A-C). And results of the semi-quantitative analysis of immunofluorescence images were presented in Fig. 9D-F. CD68 is specifically expressed by tissue macrophages which act a critical role in wound repair (Yuqing Liang et al., 2021; B. Yang et al., 2020). Herein, the inflammation in wound site was identified by CD68 immunofluorescence staining. As displayed in Fig. 9A, wounds treated with H-Ag/III showed less expression of CD68 after 7 days of treatment compared to that in the other four groups. In addition, the inflammatory response of H-Ag group was lower than that of H-C, H-III and control groups, illustrating the antibacterial activity of the AgNPs decorated hydrogels.

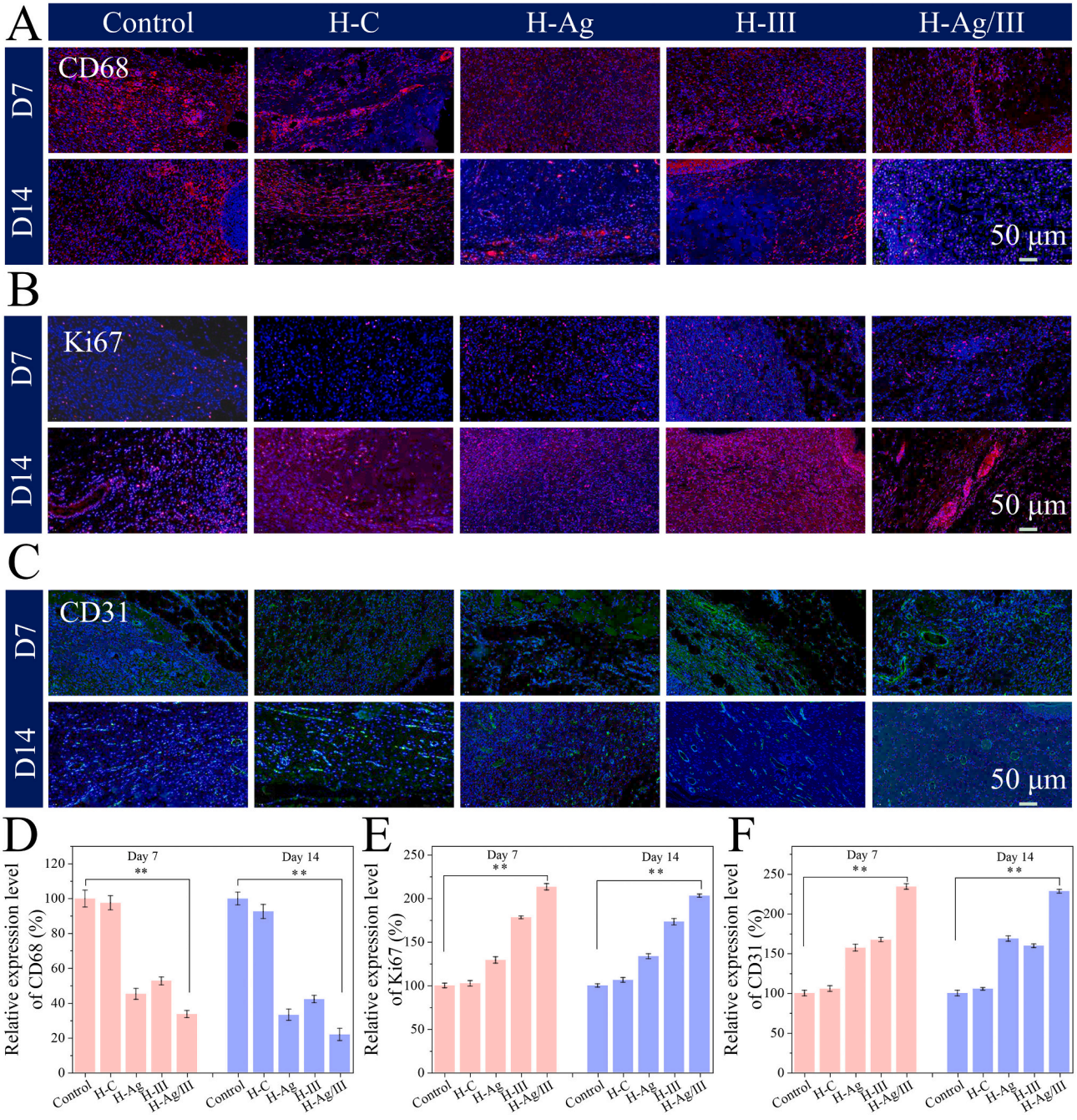

Fig. 9. Immunofluorescence images of the skin tissues labeled with CD68 (red), Ki67 (red) and CD31 (green) after different treatment at days 7 and 14. Quantitative analysis of CD68, Ki-67 and CD31 expressions after different treatment at days 7 and 14. (mean ± SD, $n = 6$, $^{**}P < 0.01$.)

Though the expression of CD68 was slightly decreased in five groups after 14 days of treatment, the inflammatory response in the H-Ag/III group was still lower than that in control and H-C groups (Fig. 9D). The above results indicated the prepared hydrogels with excellent antibacterial ability could effectively decrease the inflammatory response.

Since the cell nuclei related to mitosis can be labeled by Ki67 antibody, Ki67-positive cells may be proliferating cells, such as keratinocytes, fibroblasts, vascular endothelial cells and so on, that play certain role during wound healing. As displayed in Fig. 9B and E, the expression level of Ki67 in wounds treated with H-Ag/III hydrogel was higher than that in other four groups after 7 and 14 days of treatment. This might be due to the controlled release of rhCol III, which possessed excellent affinity for cells (Yang, Wu, et al., 2021), thus promoting cell proliferation and tissue regeneration.

Angiogenesis of the wound was evaluated by CD31 immunofluorescence staining at day 7 and day 14 post-surgery in this research. As we all know, CD31 is a key vascular endothelial cell marker and plays a vital role in vascular regeneration (Yuqing Liang et al., 2021; Suo et al., 2021; Yang, Liang, et al., 2021; L. Zhou et al., 2021). As shown in Fig. 9C, weak positive staining of CD31 was presented in the control and H-C groups. And the wounds treated with H-Ag/III appeared strongest fluorescence intensity of CD31 (green) on 7th and 14th days (Fig. 9F), revealing the advantages of the addition of rhCol III and antibacterial AgNPs in accelerating wound repair and improving angiogenesis. In summary, these results illustrated that injectable hydrogel with functions of tissue adhesion, self-healing, antioxidant, and antibacterial could effectively accelerate the repair of infected diabetic wounds by reducing the expression of CD68 and upregulating production of Ki67 and CD31 simultaneously.

4. Conclusion

In conclusion, a novel, facile and versatile strategy for the preparation of multifunctional dressings was successfully developed to promote wound repair and skin tissue regeneration in chronic diabetic wounds. The high-purity HA-DA and OMC-PBA were successfully synthesized first. And an injectable multifunctional hydrogel dressing with good biocompatibility, self-healing performance, antibacterial activity, antioxidant capacity, and tissue adhesion was designed and facilely prepared by crosslinking HA-DA with OMC-PBA. The introduction of dopamine gave the hydrogel good tissue adhesion and excellent antioxidant activity. Additionally, H-Ag/III hydrogels exhibited pH-/H_2O_2-responsive drug release profile, high-antibacterial activity against *E. coli*, *S. aureus* and could increase cell proliferation *in vitro*. Furthermore, the H-Ag/III hydrogels could significantly inhibit *in vivo* bacterial infections and accelerate wound repair in a full-thickness diabetic rat bacterial infected skin wound model. Especially, histomorphological evaluation and immunofluorescence staining of CD68, Ki67 and CD31 expression further proved the excellent promoting effects of H-Ag/III in wound repair by promoting granulation tissue formation, collagen deposition, reducing on-site inflammation, enhancing cell proliferation, and promoting angiogenesis. This research demonstrated multifunctional injectable H-Ag/III hydrogels could accelerate the repair of infected diabetic wounds. On the other hand, our work also proved that this new tailored rhCol III had a certain promoting effect in repair of chronic wounds. We also look forward to the development and application of more rhCol III products in the field of human life and health in the future.

Compliance with ethical standards

All authors declare that they have no conflict of interest.

CRediT authorship contribution statement

Lin yu Long: Investigation, Methodology, Software, Data curation, Writing – original draft. **Cheng Hu:** Investigation, Methodology, Software, Data curation, Writing – original draft. **Wenqi Liu:** Data curation. **Can Wu:** Investigation. **Lu Lu:** Investigation. **Li Yang:** Funding acquisition, Project administration, Writing – review & editing. **Yun bing Wang:** Data curation, Writing – review & editing.

Declaration of competing interest

The authors declare that they have no known competing financial interests or personal relationships that could have appeared to influence the work reported in this paper.

Acknowledgment

This work is supported by the National Natural Science Foundation of China (32101107), National Key Research and Development Programs (2017YFC1104200), the Program of Introducing Talents of Discipline to Universities (111 Project, No. B16033), the Fundamental Research Funds for the Central Universities (No. YJ2021115) and the 1·3·5 project for disciplines of excellence. Thanks to Shanxi Jinbo Bio-Pharmaceutical Co., Ltd. for help and guidance in this study. We also thank Beijing Chongyuan Yongxin Technology Co., Ltd. and Mr. Qiuju Zhou from Xinyang Normal University for their help during the experiment.

Appendix A. Supplementary data

Supplementary data to this article can be found online at https://doi.org/10.1016/j.carbpol.2022.119456.

References

Ahmadian, Z., Correia, A., Hasany, M., Figueiredo, P., Dobakhti, F., Eskandari, M. R., Hosseini, S. H., Abiri, R., Khorshid, S., Hirvonen, J., Santos, H. A., & Shahbazi, M. A. (2021). A hydrogen-bonded extracellular matrix-mimicking bactericidal hydrogel with radical scavenging and hemostatic function for pH-responsive wound healing acceleration. *Advanced Healthcare Materials, 10*(3), 1–12. https://doi.org/10.1002/adhm.202001122

Aydemir Sezer, U., Sahin, İ., Aru, B., Olmez, H., Yanıkkaya Demirel, G., & Sezer, S. (2019). Cytotoxicity, bactericidal and hemostatic evaluation of oxidized cellulose microparticles: Structure and oxidation degree approach. *Carbohydrate Polymers, 219* (March), 87–94. https://doi.org/10.1016/j.carbpol.2019.05.005

Cao, C., Yang, N., Zhao, Y., Yang, D., Hu, Y., Yang, D., Song, X., Wang, W., & Dong, X. (2021). Biodegradable hydrogel with thermo-response and hemostatic effect for photothermal enhanced anti-infective therapy. *Nano Today, 39*, Article 101165. https://doi.org/10.1016/j.nantod.2021.101165

Chen, G., Yu, Y., Wu, X., Wang, G., Ren, J., & Zhao, Y. (2018). Bioinspired multifunctional hybrid hydrogel promotes wound healing. *Advanced Functional Materials, 28*(33), 1–10. https://doi.org/10.1002/adfm.201801386

Gao, Y., Li, Z., Huang, J., Zhao, M., & Wu, J. (2020). In situformation of injectable hydrogels for chronic wound healing. *Journal of Materials Chemistry B, 8*(38), 8768–8780. https://doi.org/10.1039/d0tb01074j

He, J., Shi, M., Liang, Y., & Guo, B. (2020). Conductive adhesive self-healing nanocomposite hydrogel wound dressing for photothermal therapy of infected full-thickness skin wounds. *Chemical Engineering Journal, 394*(March), Article 124888. https://doi.org/10.1016/j.cej.2020.124888

Hu, C., Zhang, F., Long, L., Kong, Q., Luo, R., & Wang, Y. (2020a). Dual-responsive injectable hydrogels encapsulating drug-loaded micelles for on-demand antimicrobial activity and accelerated wound healing. *Journal of Controlled Release, 324*(May), 204–217. https://doi.org/10.1016/j.jconrel.2020.05.010

Hu, C., Zhang, F., Long, L., Kong, Q., Luo, R., & Wang, Y. (2020b). Dual-responsive injectable hydrogels encapsulating drug-loaded micelles for on-demand antimicrobial activity and accelerated wound healing. *Journal of Controlled Release, 324*(February), 204–217. https://doi.org/10.1016/j.jconrel.2020.05.010

Hu, C., Long, L., Cao, J., Zhang, S., & Wang, Y. (2021). Dual-crosslinked mussel-inspired smart hydrogels with enhanced antibacterial and angiogenic properties for chronic infected diabetic wound treatment via pH-responsive quick cargo release. *Chemical Engineering Journal, 411*(October 2020), Article 128564. https://doi.org/10.1016/j.cej.2021.128564

Huang, J., Jiang, Y., Liu, Y., Ren, Y., Xu, Z., Li, Z., Zhao, Y., Wu, X., & Ren, J. (2021). Marine-inspired molecular mimicry generates a drug-free, but immunogenic hydrogel adhesive protecting surgical anastomosis. *Bioactive Materials, 6*(3), 770–782. https://doi.org/10.1016/j.bioactmat.2020.09.010

Huang, J., Liu, Y., Chi, X., Jiang, Y., Xu, Z., Qu, G., Zhao, Y., Li, Z., Chen, C., Chen, G., Wu, X., & Ren, J. (2021). Programming electronic skin with diverse skin-like

properties. *Journal of Materials Chemistry A, 9*(2), 963–973. https://doi.org/10.1039/d0ta09101d

Huang, S., Liu, H., Liao, K., Hu, Q., Guo, R., & Deng, K. (2020). Functionalized GO nanovehicles with nitric oxide release and photothermal activity-based hydrogels for bacteria-infected wound healing. *ACS Applied Materials and Interfaces, 12*(26), 28952–28964. https://doi.org/10.1021/acsami.0c04080

Huerta-Angeles, G., Bobek, M., Příkopová, E., Šmejkalová, D., & Velebný, V. (2014). Novel synthetic method for the preparation of amphiphilic hyaluronan by means of aliphatic aromatic anhydrides. *Carbohydrate Polymers, 111*, 883–891. https://doi.org/10.1016/j.carbpol.2014.05.035

Huerta-Angeles, G., Brandejsová, M., Knotková, K., Hermannová, M., Moravcová, M., Šmejkalová, D., & Velebný, V. (2016). Synthesis of photo-crosslinkable hyaluronan with tailored degree of substitution suitable for production of water resistant nanofibers. *Carbohydrate Polymers, 137*, 255–263. https://doi.org/10.1016/j.carbpol.2015.10.077

Huerta-Angeles, G., Brandejsová, M., Kulhánek, J., Pavlík, V., Šmejkalová, D., Vágnerová, H., & Velebný, V. (2016). Linolenic acid grafted hyaluronan: Process development, structural characterization, biological assessing, and stability studies. *Carbohydrate Polymers, 152*, 815–824. https://doi.org/10.1016/j.carbpol.2016.07.030

Huerta-Angeles, G., Brandejsová, M., Nigmatullin, R., Kopecká, K., Vágnerová, H., Šmejkalová, D., Roy, I., & Velebný, V. (2017). Synthesis of graft copolymers based on hyaluronan and poly(3-hydroxyalkanoates). *Carbohydrate Polymers, 171*, 220–228. https://doi.org/10.1016/j.carbpol.2017.05.011

Hussain, M., Suo, H., Xie, Y., Wang, K., Wang, H., Hou, Z., Gao, Y., Zhang, L., Tao, J., Jiang, H., & Zhu, J. (2021). Dopamine-substituted multidomain peptide hydrogel with inherent antimicrobial activity and antioxidant capability for infected wound healing. *ACS Applied Materials and Interfaces, 13*(25), 29380–29391. https://doi.org/10.1021/acsami.1c07656

Hwang, C. R., Lee, S. Y., Kim, H. J., Lee, K. J., Lee, J., Kim, D. D., & Cho, H. J. (2021). Polypseudorotaxane and polydopamine linkage-based hyaluronic acid hydrogel network with a single syringe injection for sustained drug delivery. *Carbohydrate Polymers, 266*(April), Article 118104. https://doi.org/10.1016/j.carbpol.2021.118104

Khamrai, M., Banerjee, S. L., Paul, S., Ghosh, A. K., Sarkar, P., & Kundu, P. P. (2019). A mussel mimetic, bioadhesive, antimicrobial patch based on dopamine-modified bacterial cellulose/rGO/Ag NPs: A green approach toward wound-healing applications. *ACS Sustainable Chemistry and Engineering, 7*(14), 12083–12097. https://doi.org/10.1021/acssuschemeng.9b01163

Koivusalo, L., Kauppila, M., Samanta, S., Parihar, V. S., Ilmarinen, T., Miettinen, S., Oommen, O. P., & Skottman, H. (2019). Tissue adhesive hyaluronic acid hydrogels for sutureless stem cell delivery and regeneration of corneal epithelium and stroma. *Biomaterials, 225*(September), Article 119516. https://doi.org/10.1016/j.biomaterials.2019.119516

Lee, S. Y., Yang, M., Seo, J. H., Jeong, D. I., Hwang, C., Kim, H. J., Lee, J., Lee, K., Park, J., & Cho, H. J. (2021). Serially pH-modulated hydrogels based on boronate ester and polydopamine linkages for local cancer therapy. *ACS Applied Materials and Interfaces, 13*(2), 2189–2203. https://doi.org/10.1021/acsami.0c16199

Li, H., Cheng, F., Wei, X., Yi, X., Tang, S., Wang, Z., Zhang, Y. S., He, J., & Huang, Y. (2021). Injectable, self-healing, antibacterial, and hemostatic N,O-carboxymethyl chitosan/oxidized chondroitin sulfate composite hydrogel for wound dressing. *Materials Science and Engineering C, 118*(April 2020), Article 111324. https://doi.org/10.1016/j.msec.2020.111324

Li, M., Zhang, Z., Liang, Y., He, J., & Guo, B. (2020). Multifunctional tissue-adhesive cryogel wound dressing for rapid nonpressing surface hemorrhage and wound repair. *ACS Applied Materials and Interfaces, 12*(32), 35856–35872. https://doi.org/10.1021/acsami.0c08285

Li, Y., Fu, R., Duan, Z., Zhu, C., & Fan, D. (2021). Construction of multifunctional hydrogel based on the tannic acid-metal coating decorated MoS2 dual nanozyme for bacteria-infected wound healing. *Bioactive Materials*, (July)https://doi.org/10.1016/j.bioactmat.2021.07.023

Li, Z., Cao, H., Xu, Y., Li, X., Han, X. W., Fan, Y., Jiang, Q., Sun, Y., & Zhang, X. (2021). Bioinspired polysaccharide hybrid hydrogel promoted recruitment and chondrogenic differentiation of bone marrow mesenchymal stem cells. *Carbohydrate Polymers, 267*(April), Article 118224. https://doi.org/10.1016/j.carbpol.2021.118224

Liang, Y., Zhao, X., Hu, T., Chen, B., Yin, Z., Ma, P. X., & Guo, B. (2019). Adhesive hemostatic conducting injectable composite hydrogels with sustained drug release and photothermal antibacterial activity to promote full-thickness skin regeneration during wound healing. *Small, 15*(12), 1–17. https://doi.org/10.1002/smll.201900046

Liang, Y., Li, Z., Huang, Y., Yu, R., & Guo, B. (2021). Dual-dynamic-bond cross-linked antibacterial adhesive hydrogel sealants with on-demand removability for post-wound-closure and infected wound healing. *ACS Nano, 15*(4), 7078–7093. https://doi.org/10.1021/acsnano.1c00204

Lin, M., Long, H., Liang, M., Chu, B., Ren, Z., Zhou, P., Wu, C., Liu, Z., & Wang, Y. (2021). Antifracture, antibacterial, and anti-inflammatory hydrogels consisting of silver-embedded curdlan nanofibrils. *ACS Applied Materials and Interfaces, 13*(31), 36747–36756. https://doi.org/10.1021/acsami.1c06603

Liu, S., Liu, X., Ren, Y., Wang, P., Pu, Y., Yang, R., Wang, X., Tan, X., Ye, Z., Maurizot, V., & Chi, B. (2020). Mussel-inspired dual-cross-linking hyaluronic acid/ε-polylysine hydrogel with self-healing and antibacterial properties for wound healing. *ACS Applied Materials and Interfaces, 12*(25), 27876–27888. https://doi.org/10.1021/acsami.0c00782

Long, L., Liu, W., Li, L., Hu, C., He, S., Lu, L., Wang, J., Yang, L., & Wang, Y. (2022). Dissolving microneedle-encapsulated drug-loaded nanoparticles and recombinant humanized collagen type III for the treatment of chronic wound via anti-inflammation and enhanced cell proliferation and angiogenesis. *Nanoscale, 14*(4), 1285–1295. https://doi.org/10.1039/d1nr07708b

Qu, J., Zhao, X., Liang, Y., Zhang, T., Ma, P. X., & Guo, B. (2018). Antibacterial adhesive injectable hydrogels with rapid self-healing, extensibility and compressibility as wound dressing for joints skin wound healing. *Biomaterials, 183*(July), 185–199. https://doi.org/10.1016/j.biomaterials.2018.08.044

Qu, J., Zhao, X., Liang, Y., Xu, Y., Ma, P. X., & Guo, B. (2019). Degradable conductive injectable hydrogels as novel antibacterial, anti-oxidant wound dressings for wound healing. *Chemical Engineering Journal, 362*(October 2018), 548–560. https://doi.org/10.1016/j.cej.2019.01.028

Shan, M., Gong, C., Li, B., & Wu, G. (2017). A pH, glucose, and dopamine triple-responsive, self-healable adhesive hydrogel formed by phenylborate-catechol complexation. *Polymer Chemistry, 8*(19), 2997–3005. https://doi.org/10.1039/c7py00519a

Shen, S., Fan, D., Yuan, Y., Ma, X., Zhao, J., & Yang, J. (2021). An ultrasmall infinite coordination polymer nanomedicine-composited biomimetic hydrogel for programmed dressing-chemo-low level laser combination therapy of burn wounds. *Chemical Engineering Journal, 426*(June), Article 130610. https://doi.org/10.1016/j.cej.2021.130610

Suo, H., Hussain, M., Wang, H., Zhou, N., Tao, J., Jiang, H., & Zhu, J. (2021). Injectable and pH-sensitive hyaluronic acid-based hydrogels with on-demand release of antimicrobial peptides for infected wound healing. *Biomacromolecules, 22*(7), 3049–3059. https://doi.org/10.1021/acs.biomac.1c00502

Tang, Q., Chen, C., Jiang, Y., Huang, J., Liu, Y., Nthumba, P. M., Gu, G., Wu, X., Zhao, Y., & Ren, J. (2020). Engineering an adhesive based on photosensitive polymer hydrogels and silver nanoparticles for wound healing. *Journal of Materials Chemistry B, 8*(26), 5756–5764. https://doi.org/10.1039/d0tb00726a

Teng, L., Shao, Z., Bai, Q., Zhang, X., He, Y. S., Lu, J., Zou, D., Feng, C., & Dong, C. M. (2021). Biomimetic glycopolypeptide hydrogels with tunable adhesion and microporous structure for fast hemostasis and highly efficient wound healing. *Advanced Functional Materials, 31*(43), 1–11. https://doi.org/10.1002/adfm.202105628

Tsai, T. Y., Shen, K. H., Chang, C. W., Jovanska, L., Wang, R., & Yeh, Y. C. (2021). In situ formation of nanocomposite double-network hydrogels with shear-thinning and self-healing properties. *Biomaterials Science, 9*(3), 985–999. https://doi.org/10.1039/d0bm01528h

Wang, M., Wang, C., Chen, M., Xi, Y., Cheng, W., Mao, C., Xu, T., Zhang, X., Lin, C., Gao, W., Guo, Y., & Lei, B. (2019). Efficient angiogenesis-based diabetic wound healing/skin reconstruction through bioactive antibacterial adhesive ultraviolet shielding nanodressing with exosome release. *ACS Nano, 13*(9), 10279–10293. https://doi.org/10.1021/acsnano.9b03656

Wu, M., Chen, J., Huang, W., Yan, B., Peng, Q., Liu, J., Chen, L., & Zeng, H. (2020). Injectable and self-healing nanocomposite hydrogels with ultrasensitive pH-responsiveness and tunable mechanical properties: Implications for controlled drug delivery. *Biomacromolecules, 21*(6), 2409–2420. https://doi.org/10.1021/acs.biomac.0c00347

Wu, Z., Zhou, W., Deng, W., Xu, C., Cai, Y., & Wang, X. (2020). Antibacterial and hemostatic thiol-modified chitosan-immobilized AgNPs composite sponges. *ACS Applied Materials and Interfaces, 12*(18), 20307–20320. https://doi.org/10.1021/acsami.0c05430

Xiong, Y., Zhang, X., Ma, X., Wang, W., Yan, F., Zhao, X., Chu, X., Xu, W., & Sun, C. (2021). A review of the properties and applications of bioadhesive hydrogels. *Polymer Chemistry, 12*(26), 3721–3739. https://doi.org/10.1039/d1py00282a

Xu, Z., Han, S., Gu, Z., & Wu, J. (2020). Advances and impact of antioxidant hydrogel in chronic wound healing. *Advanced Healthcare Materials, 9*(5), 1–11. https://doi.org/10.1002/adhm.201901502

Yang, B., Song, J., Jiang, Y., Li, M., Wei, J., Qin, J., Peng, W., Lasaosa, F. L., He, Y., Mao, H., Yang, J., & Gu, Z. (2020). Injectable adhesive self-healing multicross-linked double-network hydrogel facilitates full-thickness skin wound healing. *ACS Applied Materials and Interfaces, 12*(52), 57782–57797. https://doi.org/10.1021/acsami.0c18948

Yang, L., Wu, H., Lu, L., He, Q., Xi, B., Yu, H., Luo, R., Wang, Y., & Zhang, X. (2021). A tailored extracellular matrix (ECM) - mimetic coating for cardiovascular stents by stepwise assembly of hyaluronic acid and recombinant human type III collagen. *Biomaterials, 276*(July). https://doi.org/10.1016/j.biomaterials.2021.121055

Yang, Y., Liang, Y., Chen, J., Duan, X., & Guo, B. (2021). Mussel-inspired adhesive antioxidant antibacterial hemostatic composite hydrogel wound dressing via photo-polymerization for infected skin wound healing. *Bioactive Materials*, (February) https://doi.org/10.1016/j.bioactmat.2021.06.014

Yao, Y., Zhang, H., Wang, Z., Ding, J., Wang, S., Huang, B., Ke, S., & Gao, C. (2019). Reactive oxygen species (ROS)-responsive biomaterials mediate tissue microenvironments and tissue regeneration. *Journal of Materials Chemistry B, 7*(33), 5019–5037. https://doi.org/10.1039/c9tb00847k

Yu, N., Wang, X., Qiu, L., Cai, T., Jiang, C., Sun, Y., Li, Y., Peng, H., & Xiong, H. (2020). Bacteria-triggered hyaluronan/AgNPs/gentamicin nanocarrier for synergistic bacteria disinfection and wound healing application. *Chemical Engineering Journal, 380*(235), Article 122582. https://doi.org/10.1016/j.cej.2019.122582

Zhang, K., Jiao, X., Zhou, L., Wang, J., Wang, C., Qin, Y., & Wen, Y. (2021). Nanofibrous composite aerogel with multi-bioactive and fluid gating characteristics for promoting diabetic wound healing. *Biomaterials, 276*(July), Article 121040. https://doi.org/10.1016/j.biomaterials.2021.121040

Zhao, H., Huang, J., Li, Y., Lv, X., Zhou, H., Wang, H., Xu, Y., Wang, C., Wang, J., & Liu, Z. (2020). ROS-scavenging hydrogel to promote healing of bacteria infected diabetic wounds. *Biomaterials, 258*(August), Article 120286. https://doi.org/10.1016/j.biomaterials.2020.120286

Zhao, L., Niu, L., Liang, H., Tan, H., Liu, C., & Zhu, F. (2017). PH and glucose dual-responsive injectable hydrogels with insulin and fibroblasts as bioactive dressings for diabetic wound healing. *ACS Applied Materials and Interfaces, 9*(43), 37563–37574. https://doi.org/10.1021/acsami.7b09395

Zhao, X., Wu, H., Guo, B., Dong, R., Qiu, Y., & Ma, P. X. (2017). Antibacterial anti-oxidant electroactive injectable hydrogel as self-healing wound dressing with hemostasis and adhesiveness for cutaneous wound healing. *Biomaterials, 122*, 34–47. https://doi.org/10.1016/j.biomaterials.2017.01.011

Zhao, X., Guo, B., Wu, H., Liang, Y., & Ma, P. X. (2018). Injectable antibacterial conductive nanocomposite cryogels with rapid shape recovery for noncompressible hemorrhage and wound healing. *NatureCommunications, 9*(1). https://doi.org/10.1038/s41467-018-04998-9

Zheng, Z., Bian, S., Li, Z., Zhang, Z., Liu, Y., Zhai, X., Pan, H., & Zhao, X. (2020). Catechol modified quaternized chitosan enhanced wet adhesive and antibacterial properties of injectable thermo-sensitive hydrogel for wound healing. *Carbohydrate Polymers, 249*(August), Article 116826. https://doi.org/10.1016/j.carbpol.2020.116826

Zhong, X., Tong, C., Liu, T., Li, L., Liu, X., Yang, Y., Liu, R., & Liu, B. (2020). Silver nanoparticles coated by green graphene quantum dots for accelerating the healing of: MRSA-infected wounds. *Biomaterials Science, 8*(23), 6670–6682. https://doi.org/10.1039/d0bm01398f

Zhou, D., Li, S., Pei, M., Yang, H., Gu, S., Tao, Y., Ye, D., Zhou, Y., Xu, W., & Xiao, P. (2020). Dopamine-modified hyaluronic acid hydrogel adhesives with fast-forming and high tissue adhesion. *ACS Applied Materials and Interfaces, 12*(16), 18225–18234. https://doi.org/10.1021/acsami.9b22120

Zhou, L., Zheng, H., Liu, Z., Wang, S., Liu, Z., Chen, F., Zhang, H., Kong, J., Zhou, F., & Zhang, Q. (2021). Conductive antibacterial hemostatic multifunctional scaffolds based on Ti3C2TxMXene nanosheets for promoting multidrug-resistant bacteria-infected wound healing. *ACS Nano, 15*(2), 2468–2480. https://doi.org/10.1021/acsnano.0c06287